A Novel Framework for Quantitatively Connecting the Mechanical Design of Passive Prosthetic Feet to Lower Leg Trajectory

Kathryn M. Olesnavage and Amos G. Winter, V, *Member, IEEE*

***Abstract*— This paper presents a novel framework that quantitatively connects the mechanical design of a prosthetic foot to its anticipated biomechanical performance. The framework uses kinetic inputs (ground reaction forces and center of pressure) to predict kinematic outputs of the lower leg segment by knowing the geometry and stiffness of the foot. The error between the predicted and target kinematics is evaluated using a root-mean-square error function called the Lower Leg Trajectory Error (LLTE). Using physiological kinetic inputs and kinematic targets, three model foot architectures were optimized to minimize the LLTE. The resulting predicted lower leg kinematics were compared to those of the same foot architectures optimized for physiological roll-over geometry. The feet with minimized LLTE had lower leg kinematics closer to physiological than those optimized for roll-over geometry. A prosthetic foot that exactly mimics physiological roll-over geometry may result in gait kinematics that differ greatly from physiological, as roll-over geometry omits information about the foot-ground contact constraint, lower leg orientation, and temporal progression of a step. The LLTE-based framework is agnostic to specific foot designs provided their constitutive behavior can be characterized, and it can accept alternate inputs and targets depending on what performance and clinical objectives are desired.**

***Index Terms*— Biomechanics, energy storage and return, lower leg trajectory error, prosthetic feet, prosthetics, roll-over geometry.**

I. Introduction

THERE is substantial evidence to suggest that the mechanical function of passive below-knee prostheses affects walking mechanics and efficiency of users [1]–[9]. However, multiple reviews of the literature have concluded that *how* the mechanical features of a passive prosthesis affect the functionality is not fully understood [9]–[12]. Without this knowledge, passive prosthetic feet cannot be quantitatively optimized for peak performance and desired behaviors.

Manuscript received November 6, 2017; revised February 19, 2018; accepted April 8, 2018. Date of publication June 18, 2018; date of current version August 7, 2018. This work was supported by the Tata Center for Technology and Design, MIT. *(Corresponding author: Amos G. Winter.)*

The authors are with the Global Engineering and Research Laboratory, Department of Mechanical Engineering, Massachusetts Institute of Technology, Cambridge, MA 02139 USA (e-mail: kolesnav@mit.edu; awinter@mit.edu).

Digital Object Identifier 10.1109/TNSRE.2018.2848845

The most recent of the aforementioned literature reviews categorized the mechanical characterization of prosthetic feet into two approaches: lumped parameter models and roll-over models [12]. Lumped parameter models use discrete viscoelastic properties, such as stiffness and damping coefficients, to represent the foot. These properties are measured at particular locations on the foot and under specified loading scenarios. There is no consensus on which viscoelastic properties should be measured or how many different discrete load scenarios should be considered. Typically only one or two are presented, often for a load applied to the forefoot, the heel, or both, but these are inadequate to capture the behavior of the foot across all of stance phase [12]. One study addressed this by using 66 independent, one degree-of-freedom spring and damper models to represent the full behavior of the foot, but doing so loses the simplicity that makes the lumped parameter approach desirable [13]. Only recently has work been done to measure the viscoelastic properties of a biological foot/ankle complex so that the results can be incorporated into prosthetic foot design [14]. Prior to this work, most studies measured the viscoelastic properties of existing commercially available feet, and either replicated and varied those properties with experimental prototypes for clinical testing, or simply tested a variety of commercially available feet after having measured these properties, and empirically drew conclusions about the affect of the lumped parameter values on the biomechanical performance [5], [15]–[19]. However, these results cannot be assumed to be generally applicable until it is shown that the lumped parameters used are sufficient to fully capture the behavior of any prosthetic foot.

Roll-over geometry models are more comprehensive, as they incorporate the behavior of the foot throughout all of stance phase rather than at a few discrete instants. The roll-over geometry of a foot is defined as the path of the center of pressure along the foot in the ankle-knee reference frame during the single-limb stance phase [20]. Studies have suggested that prosthetic feet that replicate roll-over geometry result in increased metabolic efficiency, more symmetric gait, and higher subjective preference [3], [4], [20]–[22]. However, as will be discussed in the following section, roll-over geometry has limitations that make it insufficient as a

design objective in optimizing the mechanical properties of prosthetic feet.

This study proposes a novel framework that connects the mechanical design of a prosthetic foot to its biomechanical functionality by applying an assumed set of loads on an analytical model of a prosthetic foot and calculating the deformation under those loads. Then the deformed shape of the foot at each time interval during stance is used to obtain the trajectory of the lower leg segment under those assumed loads. A cost function, which we have called the Lower Leg Trajectory Error (LLTE), quantifies how far this calculated lower leg trajectory is from a target trajectory. The cost function can be used to optimize the mechanical design of a prosthetic foot to best replicate the target lower leg trajectory under the applied loads. Our framework provides an advantage on lumped parameter models by incorporating all of stance phase, and by directly connecting the mechanical properties of a prosthetic foot to its biomechanical performance using fundamental physics. This approach to prosthetic foot design also provides advantages to roll-over geometry by accounting for the deformation within the foot at each time interval during stance and the foot's kinematic constraints with the ground, which are necessary factors to determine the relative orientation between the lab reference frame and the ankle-knee reference frame.

The LLTE-based framework for optimizing the design of prosthetic feet was first introduced and demonstrated as a design objective on a single prosthetic foot architecture at the 2015 IEEE ICORR [23]. This paper builds on our previous work by improving the original definition of the LLTE, expanding the optimization to multiple prosthetic foot architectures, and comparing the results to the same architectures optimized for roll-over geometry.

II. Roll-Over Geometry and Leg Orientation

The goal of a passive prosthesis is to replicate biological limb functionality with a relatively simple mechanical structure. For a passive mechanical prosthesis, a given loading scenario will produce a specific deformed shape. The relationship between the loading and the deformation, or the stiffness, can be non-linear and/or vary in different parts of the structure, but even in these complex situations, the deformation resulting from a specific load can always be calculated.

Similar to stiffness, the roll-over geometry of a prosthetic foot is a measure of the shape of the foot in response to loading. When the center of pressure is at a certain position along the foot, the roll-over geometry shows the vertical deflection of that point in response to the corresponding ground reaction forces. The roll-over geometry also serves to simplify the many variables that can be measured during a biological step into a single curve that can be used as a design objective.

While the roll-over geometry compiles a lot of information into a single curve, it does not provide any information regarding the orientation of the lower leg segment in the laboratory reference frame (Fig. 1). When the center of pressure is located at a particular point along the roll-over geometry, that single

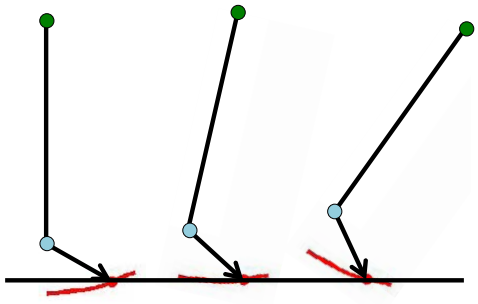

Fig. 1. For a below-knee prosthesis (shown here with the green dot representing the user's knee, blue dot representing the ankle) for which all that is known is the roll-over geometry (red curve), when the center of pressure is at a particular location (red dot), the orientation of the lower leg segment is indeterminable.

point does not constrain the angular orientation of the foot-ankle-knee complex. More information is needed about the physical construction of the foot and how it interacts with the ground to fully define the orientation of the system.

A person with a transtibial amputation interfaces with the prosthesis through the socket. Throughout this work, it is assumed that there is no relative motion between the user and the socket, and that the socket and pylon are perfectly rigid. Under these assumptions, the position and orientation of the socket dictates the position and orientation of the user's residual limb. Both the socket and the residual limb make up the lower leg. In reality, there will be some motion between the residual limb and the socket primarily along the direction of the ankle-knee axis, but this motion is negligible relative to the motion of the lower leg as a whole during stance phase. The socket also transmits forces and moments to the user (Fig. 2). The orientation of the socket defines the moment arm from the ground reaction forces to the user's residual limb and knee. Therefore any variation in the orientation of the lower leg affects both the gait kinematics and the loading at the user's knee.

The physical geometry of a prosthetic foot introduces additional constraints. Typically, the foot and ground must be in contact at the instantaneous center of pressure, and no part of the foot can ever intersect the ground. For a particular foot geometry with known mechanical behavior, these constraints fully define the orientation of the lower limb. For example, consider a rigid foot, such as cut from a block of wood, shaped so that it exactly replicates the roll-over geometry of a physiological foot-ankle complex as obtained from published gait data [24]. Because no deformation occurs within the foot, the shape of the bottom of the foot determines the roll-over geometry, which makes rigid feet a useful tool to investigate different roll-over geometries [21], [22]. During stance phase, the ground must be tangent to the foot at the instantaneous center of pressure. Any other orientation would result in the foot intersecting the ground. If the center of pressure progresses forward along the ground at the same rate as in the physiological step, and if no slipping occurs between the foot and the ground, the trajectory of the foot-ankle-knee system can be found from simple geometry and compared to physiological lower leg kinematics (Fig. 3). Even though the feet in Fig. 3 have identical roll-over geometries, the resulting

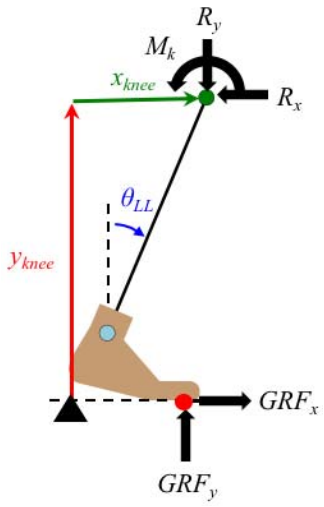

Fig. 2. Free-body diagram of a foot-ankle-knee system in the sagittal plane. The system is acted on by the ground reaction forces (GRF_x and GRF_y) and the reaction loads (R_x and R_y) and moment (M_k) at the knee. The position and orientation of the lower leg segment is fully defined by three variables: the horizontal and vertical position of the knee (x_{knee} and y_{knee}, respectively) and the angle of the lower leg with respect to vertical (θ_{LL}). The orientation of the lower limb affects not only the gait kinematics of the user, but also the reaction loading on his or her residual limb and at the knee.

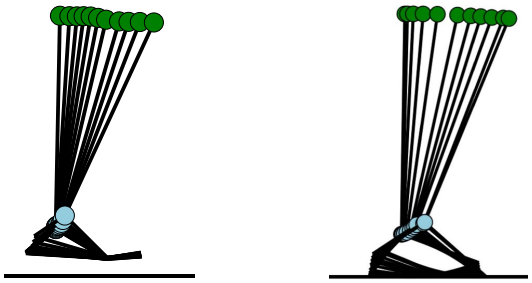

(a) (b)

Fig. 3. Lower leg kinematics of (a) a physiological foot-ankle-knee system [24], and (b) a rigid foot shaped such that the roll-over geometry is identical to that of the physiological system. While the roll-over geometries match exactly, the orientations of the roll-over geometries with respect to the ground do not, resulting in different kinematics.

lower leg kinematics differ due to the articulation inherent to the physiological foot as opposed to the rigid foot. The roll-over geometries match exactly, but the orientations of the roll-over geometries differ, resulting in different kinematics.

The additional constraints imposed by the physical embodiment of a prosthetic foot can be included in modeling to optimize the design of a given foot not only for roll-over geometry, but also for the orientation of the roll-over geometry in the laboratory reference frame, and thus the trajectory of the lower leg.

III. Framework for Replicating Lower Leg Trajectory Under Input Loads

The framework presented here consists of predicting the lower leg trajectory for a model prosthetic foot under an input set of loading data, then comparing that trajectory to a target set of lower leg trajectory data. By defining a cost function that quantifies the net difference between the model and target trajectories, the Lower Leg Trajectory Error, this approach can be used to optimize the mechanical design of a prosthetic foot to best replicate the target lower leg trajectory under the input set of loads. This concept can be described by thinking of a below-knee prosthesis as a black box attached to the user's residual limb. If this black box moves through space in such a way as to position the user's knee and lower leg correctly, it will enable natural gait kinematics for the lower leg segment, which in turn allows all body segments proximal to the lower leg to also follow natural trajectories. In reality, a passive prosthesis is a compliant structure. Given the loads on a particular structure, the resulting deformed shape of that structure can be calculated analytically for simple structures, or with finite element analysis for more complex structures. The authors propose that a goal of passive prosthetic foot design should be to create a structure that, when acted upon by typical loads as measured during gait analysis, deforms in such a way as to replicate target kinematics. The LLTE provides a measurement of how well a particular prosthesis accomplishes this goal. The idealized black box that produces exactly the target kinematics under the input loading would have an LLTE $= 0$. A passive prosthesis will never be able to exactly reproduce physiological lower leg trajectory because it cannot output more energy than it stores (as a physiological ankle does); but using physiological kinematics as a target and optimizing for minimal LLTE may produce a foot design that comes closest.

To calculate the lower leg trajectory for a particular prosthetic foot model, an input set of kinetic data, that is, ground reaction forces and center of pressure progression along the ground, is required, as well as a set of target kinematic data to which the simulated kinematic results can be compared. Throughout this work, a set of published gait data for a single step from an able-bodied subject provides both the input kinetic data and the target output kinematic data [24].

In using able-bodied gait data for the target kinematics as is done in this work, it is implicitly assumed that symmetric gait and physiological ground reaction forces are optimal. Some recent work suggests that symmetric gait kinematics may not be metabolically optimal for persons with unilateral transtibial amputations [25]. According to these studies, the objective of prosthetic foot design should not be to reproduce symmetric, able-bodied gait kinematics if the clinical goal is to minimize the metabolic cost of walking. However, there are both social and biomechanical reasons to target symmetric gait. From a social standpoint, gait asymmetries may draw unwanted attention to the fact that someone uses a prosthesis. From the authors' experience working with Bhagwan Mahaveer Viklang Sahayata Samiti (BMVSS) of Jaipur, India, the largest distributor of prosthetic limbs in the world, amputees in poor countries want to appear as able-bodied as possible to avoid stigmas against disability. Many of BMVSS's patients choose to use a heavy cosmesis over their endoskeletal pylon to better hide their prosthesis, despite the fact that the added mass decreases the metabolic efficiency of walking. Another argument for targeting symmetric gait kinematics and ground

loading is to minimize the risk of injuries related to long-term prosthesis use [26]. To the authors' knowledge, no studies advocating for targeting asymmetric gait have investigated these long-term consequences.

To define the position of the lower leg in the sagittal plane for a kinematic simulation of a given prosthesis model, three variables, x_{knee}^{model}, y_{knee}^{model}, and θ_{LL}^{model}, are needed (Fig. 2). These can then be compared to target kinematic values taken from published physiological gait data, x_{knee}^{phys}, y_{knee}^{phys}, and θ_{LL}^{phys}. Because the lower leg moves throughout a step, each of these variables are functions of time. The cost function, or LLTE, is defined as a root-mean-square error between the predicted lower leg trajectory for a modeled prosthetic foot and the target lower leg trajectory data, where each component is normalized by the mean value of that component in the physiological data set. That is,

$$LLTE \equiv \left[\frac{1}{N}\sum_{n=1}^{N}\left\{\left(\frac{x_{knee,n}^{model}-x_{knee,n}^{phys}}{\bar{x}_{knee}^{phys}}\right)^2+\left(\frac{y_{knee,n}^{model}-y_{knee,n}^{phys}}{\bar{y}_{knee}^{phys}}\right)^2+\left(\frac{\theta_{LL,n}^{model}-\theta_{LL,n}^{phys}}{\bar{\theta}_{LL}^{phys}}\right)^2\right\}\right]^{\frac{1}{2}}, \quad (1)$$

where the subscript n refers to the n^{th} time interval and N is the total number of time intervals considered. The variables $\bar{x}_{knee}^{phys}$, $\bar{y}_{knee}^{phys}$, and $\bar{\theta}_{LL}^{phys}$ are the average values of each of the physiological parameters over the portion of the step included in the optimization and serve to normalize the error in each parameter. Smaller LLTE values signify a better fit with the able-bodied ankle-knee trajectory; a model that fit the data exactly would result in an LLTE value of zero.

The definition of LLTE in Eq. 1 differs from the original definition presented at the 2015 IEEE ICORR by 1) using the position of the knee rather than the ankle, and 2) normalizing the error in each parameter by the average physiological value rather than the range of physiological values [23]. A detailed explanation of the rationale for this particular cost function definition is provided in Appendix. However, the emphasis of this study is the framework to connect the mechanical design of a prosthetic foot to its biomechanical performance and a means of optimizing feet to replicate a target lower leg trajectory under given loads, rather than on the definition of the cost function or the resulting specific optimal designs presented herein.

Although the LLTE error function is evaluated using only kinematic values, it encompasses the full kinematic, kinetic, and temporal information of the lower leg, as well as the mechanical design of the foot; x_{knee}^{model}, y_{knee}^{model}, and θ_{LL}^{model} are calculated from the input GRFs acting on a foot of prescribed stiffness and geometry, and the error is determined at each point in time n during stance phase. Furthermore, it is important to note that a compliant structure, such as a prosthetic foot, defines a relationship between loads and motion. Within the framework presented here, forces are used as inputs to calculate the output motion. Similarly, the physiological motion could be used as inputs to calculate the output loading. Even though the loading on the foot is assumed and the motion calculated, this framework produces a prosthetic foot that comes as close as possible to enabling the user to replicate both physiological loading and motion, within the limitations of a specific foot's mechanical design (such as degrees of freedom, joint stiffness, etc.). The assumed loading, which is necessary to calculate the LLTE value for the foot, does not mean that a person with a transtibial amputation is expected to exert this exact loading on any foot he or she uses. In fact, this will almost certainly not be the case. But it can be said that if, under physiological loading, a prosthetic foot deforms such that the lower leg follows a trajectory far from physiological (i.e. the foot has a high LLTE value), then the only way the user will be able to walk with typical kinematics while using that foot would be to diverge from physiological loading. With that same foot, the user could only walk with physiological loading if the lower leg kinematics diverged from physiological. In reality, it is expected that the user would compensate using such a foot with changes in both loading and kinematics. Optimizing a foot for minimal LLTE value is intended to find the foot that is the least disruptive to what the rest of the user's body was designed to do during walking, in terms of both loading and motion.

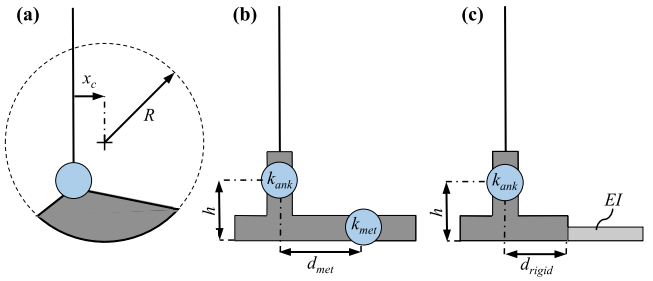

Fig. 4. Three analytical prosthetic foot architectures optimized and compared using LLTE: (a) rigid model, (b) rotational ankle and metatarsal model, and (c) rotational ankle, beam forefoot model.

IV. Design Optimization

A. Model Foot Architecture

To demonstrate the usefulness of the LLTE as a design objective, three different conceptual foot models were optimized for lower leg trajectory. The first model was a rigid foot with a circular arc forming the bottom (Fig. 4a), as used in Adamczyk's roll-over geometry studies [21], [22]. The design variables that could be varied to minimize the LLTE were the radius of the circular arc, R, and the horizontal position of the center of the circle, x_c. The vertical position of the center of the circle was determined by the length of the prosthesis from floor to knee when the lower leg segment is vertical.

The second model had rotational joints at the ankle and metatarsal, which replicated the articulated joints of biological feet (Fig. 4b). The design variables were the rotational stiffnesses of the ankle and metatarsal joints, k_{ank} and k_{met}, respectively. The links connecting these joints were modeled as perfectly rigid. The geometry of the foot, defined by the height of the center of rotation of the ankle joint, h, and the horizontal distance from the ankle to the metatarsal joint, d_{met}, was based on physiological data and held constant throughout the optimization [24].

The third model consisted of a rotational joint at the ankle, but rather than a rotational metatarsal joint, it had a cantilever beam forefoot (Fig. 4c). For this model, the design variables were the ankle stiffness, k_{ank}, and the forefoot beam bending stiffness, EI. The beam bending stiffness is the product of the elastic modulus of the beam material, E, and the second area moment of inertia of the beam cross-section, I. By considering the product as a whole rather than the components individually, the mechanical behavior of the beam can be optimized without constraining the design to any particular material. As with the jointed ankle and metatarsal model, the geometry of the foot, that is, the height of the ankle joint, h, and the horizontal length of the rigid structure from the ankle joint, d_{rigid}, was based on the location of the ankle and metatarsal joints in the physiological data and was held fixed throughout the optimization.

B. Lower Leg Trajectory Error Calculation and Optimization

To find the predicted lower leg trajectory for each foot architecture, the horizontal and vertical components of the ground reaction forces and the position of the center of pressure along the ground were used as inputs. The published gait data from which these inputs were obtained for this study were collected during a single step for a subject of body mass 56.7 kg [24]. Consequently, all results are specific to these particular data, but the method could similarly be applied to normative data. Because the purpose of this work is to demonstrate the usefulness of the LLTE in evaluating and comparing prosthetic foot models rather than to actually design a prosthetic foot, this does not affect the merit of the work. Using the published ground reaction forces and position of center of pressure as inputs, the resulting deformed shape of the foot-ankle complex and subsequent lower leg trajectory was calculated for each foot model for the portion of stance starting when the orientation of the lower leg segment relative to vertical in the physiological data set, θ_{LL}^{phys}, becomes greater than zero, and ending when the metatarsal joint marker in the published data set lifts off the ground at the end of stance. Before and after these times, the two articulated foot models are in point contact with the ground either at the very end of the heel or the toe, and can rotate about these contact points. As such, the position of the lower leg segment at these points cannot be calculated from the ground reaction force and center of pressure data without making additional assumptions. The position of the lower leg segment could be calculated for the rigid circular foot during early stance, when $\theta_{LL}^{phys} < 0$, but for the sake of comparison with the other two models, this was not included here. The following subsections describe the calculation of the deformed shape of the foot-ankle complex and lower leg trajectory for each foot model.

1) Rigid Foot: By definition, the shape of the rigid foot does not change under any applied load. Thus the only input required to calculate the lower leg trajectory for the rigid foot is the location of the center of pressure along the ground throughout the step. If no slipping occurs between the foot and the ground, then the progression of the center of pressure along the ground, $x_{cp,g}$, must be equal to the progression of the center of pressure along the bottom arc of the foot (Fig. 5a). The orientation of the lower leg, θ_{LL}, was calculated for each time interval during the step as

$$\theta_{LL} = \frac{x_{cp,g} - x_c}{R}. \tag{2}$$

The corresponding position of the instantaneous center of pressure on the foot in the ankle-knee reference frame with the origin at the intersection of the ankle-knee axis and the ground when $\theta_{LL} = 0$ is defined as $(x_{cp,f},\ y_{cp,f})$, where

$$x_{cp,f} = x_c + R\sin\theta_{LL} \tag{3}$$

and

$$y_{cp,f} = R(1 - \cos\theta_{LL}). \tag{4}$$

In the actual orientation, the instantaneous center of pressure on the ground and on the foot must coincide. Further, the ground must be tangent to the foot at this instantaneous center of pressure (Fig. 5b). The x_{knee} and y_{knee} position of the knee in the laboratory reference frame was determined for each time interval by calculating θ_{LL} from Eq. (2), rotating the foot-ankle-knee system by θ_{LL} by multiplying the array of coordinate points of the model in the ankle-knee reference frame by the rotation matrix, then translating the rotated system such that the instantaneous center of pressure on the foot was coincident with the instantaneous center of pressure on the ground. Once the lower leg position and orientation coordinates were found for each time interval from midstance to toe off, the LLTE value was calculated using Eq. (1) for the particular selection of design variables, x_c and R. This was repeated for a range of design variable values to find the set with the lowest LLTE value. The range of values for each design variable was selected by sampling the feasible design space, that is, $R > 0$ and $-R \le x_c \le R$, at a course resolution, then reducing the range and increasing the resolution in the vicinity of the design variable values yielding the mimimum LLTE value. The resulting ranges of design variable values sampled at high resolution were $-0.07\text{ m} \le x_c \le 0.08\text{ m}$ and $0.1\text{ m} \le R \le 0.9\text{ m}$.

2) Rotational Ankle and Metatarsal Foot: The geometry of this foot was selected to approximately match the locations of the joint center of rotations of the subject of Winter's gait data, with $h = 8$ cm and $d_{met} = 10.5$ cm (Fig. 4b) [24].

A free-body diagram for a particular instant during a step is depicted in Fig. 5c. It can be shown geometrically that

$$\theta_{LL} = \theta_{ank} + \theta_{met}, \tag{5}$$

where θ_{LL} is the angle of the lower leg segment as previously defined and θ_{ank} and θ_{met} are the angles of the ankle and metatarsal joints, respectively. For constant rotational joint stiffnesses k_{ank} and k_{met}, the joint angles are given by

$$\theta_{ank} = \frac{M_{ank}}{k_{ank}} \tag{6}$$

and

$$\theta_{met} = \frac{M_{met}}{k_{met}}, \tag{7}$$

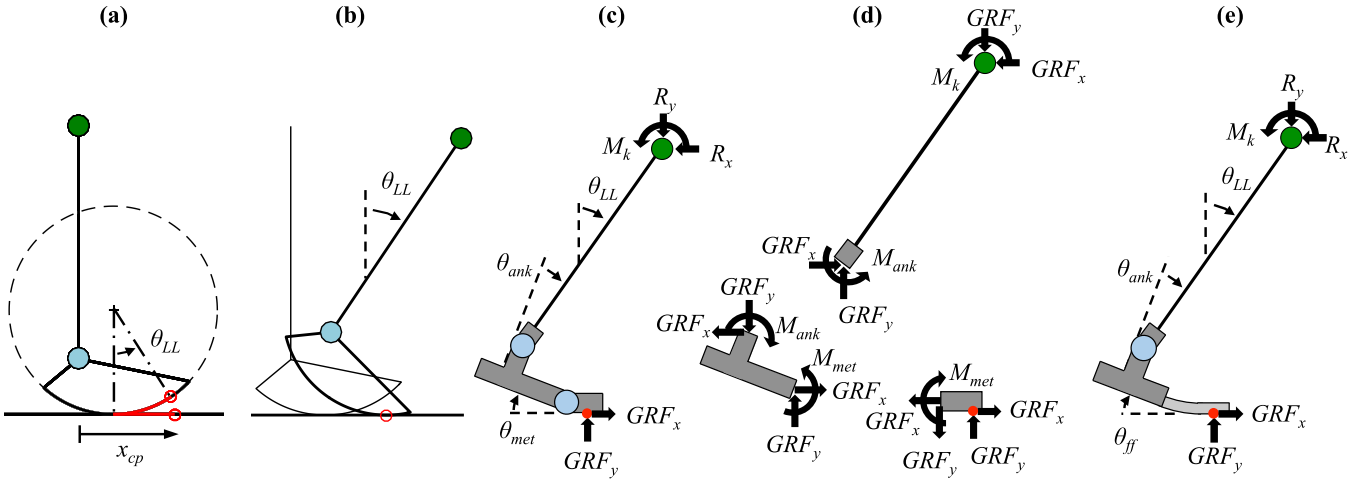

Fig. 5. Free-body diagrams of the foot models considered. (a) For the rigid foot, under a no-slip assumption the distance progressed by the center of pressure along the ground and along the bottom of the foot, shown here in red, must be equal. The instantaneous position of the center of pressure, x_{cp}, was obtained from published gait data and used as an input to calculate the lower leg trajectory [24]. (b) The orientation of the lower leg was calculated by rotating the foot-ankle-knee model by θ_{LL}, then translating the rotated model such that the location of the center of pressure on the foot and on the ground were coincident. (c) Free-body diagram of the rotational ankle and metatarsal foot's knee-ankle-foot system at a particular instant during stance. (d) Free-body diagrams showing reaction loads and moments at the metatarsal and ankle joints when the center of pressure is distal to the metatarsal joint. Under the quasistatic assumption, the joint moments and angles can be calculated from the ground reaction forces and position of the center of pressure for a given set of joint stiffnesses. (e) Free-body diagram of the knee-ankle-foot system for the rotational ankle, beam forefoot model at a particular instant during stance.

where M_{ank} and M_{met} are the moments at each of the joints produced by the ground reaction forces.

Assuming quasistatic loading and neglecting the mass of the prosthesis, equilibrium equations were used to find the joint moments as functions of the ground reaction forces and foot geometry. When the center of pressure is proximal to the metatarsal joint, the moments are

$$M_{met} = 0 \tag{8}$$

and

$$M_{ank} = GRF_y \cdot x_{cp} + GRF_x \cdot h. \tag{9}$$

When the center of pressure is distal to the metatarsal (Fig. 5d), these equations become

$$M_{met} = GRF_y \cdot \left(x_{cp} - d_{met}\right) \tag{10}$$

and

$$M_{ank} = M_{met} + GRF_y \cdot \left(d_{met}\cos\theta_{met} - h\sin\theta_{met}\right) + GRF_x \cdot \left(d_{met}\sin\theta_{met} + h\cos\theta_{met}\right). \tag{11}$$

Using equations (5) through (11) and the inputs from typical walking as previously described, the angle of the lower leg segment was calculated for a particular set of joint stiffness values to obtain θ_{LL} for each time interval. The position of the knee at each time, given by x_{knee} and y_{knee}, was found geometrically from the deformed shape of the prosthesis and the instantaneous location of the center of pressure in the global reference frame, and by assuming no slipping occurred between the bottom of the foot and the ground.

For each set of joint stiffnesses, k_{ank} and k_{met}, from a range of feasible values, $x_{knee,n}$, $y_{knee,n}$ and $\theta_{LL,n}$ were found using the above equations and then used to calculate the LLTE value. This was repeated for each set of joint stiffnesses in the range 2.0 N·m/deg $\leq k_{ank} \leq$12.0 N·m/deg and 1.2 N·m/deg $\leq k_{met} \leq$12.0 N·m/deg to find optimal stiffness values to minimize the LLTE. As was done for the rigid foot, the ranges of values were selected to encompass the set of feasible design variable values with the minimum LLTE, where feasible values in this case were $k_{ank} > 0$ and $k_{met} > 0$.

3) Rotational Ankle, Beam Forefoot Foot: As with the rotational ankle and metatarsal foot, the geometry of the rotational ankle, beam forefoot foot was selected to replicate the articulation of the physiological foot-ankle complex, with $h = 8$ cm and $d_{rigid} = 9.3$ cm [24]. The rigid structure length, d_{rigid}, was chosen such that during late stance, the effective rotational joint of the pseudo-rigid-body model of the cantilever beam forefoot would be approximately at the center of rotation of the metatarsal joint for the physiological data. The pseudo-rigid-body model approximates a cantilever beam with a vertical end load as a rigid link and a rotational joint with stiffness related to the beam bending stiffness [27].

A free-body diagram for the rotational ankle, beam forefoot model is shown in Fig. 5e. When the instantaneous center of pressure is in the rigid portion of the foot ($x_{cp} < d_{rigid}$), the model behaves exactly as the rotational ankle and metatarsal model. The moment about the ankle, M_{ank}, and the orientation of the lower leg, θ_{LL}, can therefore be calculated with Eqs. (6) and (9).

When the ground reaction forces act on the cantilever beam, the analysis is more complex. The inputs used throughout this study are the horizontal and vertical ground reaction forces in the lab reference frame. In calculating the deformed shape of the cantilever beam forefoot, it is necessary to know the relative orientation between the ground and the beam (θ_{ff} in Fig. 5e), so that the ground reaction forces can be decomposed into loads acting transverse and axial to the beam. However,

θ_{ff} cannot be found without knowing the transverse load on the beam. Thus the deformed shape of the beam was computed iteratively. Initially, it was assumed that $\theta_{ff} = 0$, so that the transverse load on the beam, F_{trans}, was equal to the vertical ground reaction force in the lab frame,

$$F_{trans} = GRF_y. \tag{12}$$

The resulting angle of the deformed beam at the point of action of the load was found with

$$\theta_{ff} = \tan^{-1}\left(\frac{F_{trans}(x_{cp} - d_{rigid})^2}{2EI}\right). \tag{13}$$

The transverse load on the beam was then calculated with the new θ_{ff},

$$F_{trans} = GRF_y \cdot \cos\theta_{ff} - GRF_x \cdot \sin\theta_{ff}. \tag{14}$$

The new F_{trans} was then used with Eq. (13) to obtain a new θ_{ff}, and so on until the difference between subsequent values of θ_{ff} was less than 0.5 degrees.

Once the orientation of the forefoot with respect to the ground, θ_{ff}, was obtained for the deformed foot, the moment about the ankle was calculated as

$$M_{ank} = GRF_y \cdot \left(x_{cp}\cos\theta_{ff} - (h-\delta)\sin\theta_{ff}\right) + GRF_x \cdot \left(x_{cp}\sin\theta_{ff} + (h-\delta)\cos\theta_{ff}\right), \tag{15}$$

where δ is the transverse deflection of the beam at the point of application of the force, that is,

$$\delta = \frac{F_{trans}x_{cp}^3}{3EI}. \tag{16}$$

The angle at the ankle joint, θ_{ank}, was then found using Eq. (6). Similar to Eq. (5) for the rotational ankle and metatarsal foot, the orientation of the lower leg segment was given by

$$\theta_{LL} = \theta_{ank} + \theta_{ff}. \tag{17}$$

The x- and y-coordinates of the knee were found using the deformed geometry of the prosthesis model and by applying the no slip assumption between the floor and the foot. For each ankle and beam bending stiffness, x_{knee}, y_{knee}, and θ_{LL} were calculated for all times from foot flat to late stance. The LLTE value for that particular set of design variables was then calculated using Eq. (1). This was repeated for each combination of design variable values in the range 3.0 N·m/deg $\leq$ k_{ank} $\leq$ 8.0 N·m/deg and 1.0 N·m^2 $\leq$ EI $\leq$ 20.0 N·m^2. These ranges were selected following the same method described for the preceding foot architectures.

C. Roll-Over Geometry Calculation and Optimization

The roll-over geometries for each foot architecture were calculated using a similar analysis as described in the previous sections. The deformed shape of each foot was found just as for the LLTE calculation, but rather than using this to obtain the position and orientation of the lower leg, it was used to find the position of the center of pressure on the deformed foot in the ankle-knee reference frame, which provided a single point on the roll-over curve for that foot. Repeating this for all times from foot flat to late stance gave the roll-over geometry for that portion of stance. The least squares error between the resulting roll-over geometry and the target roll-over geometry from the physiological data was then calculated. Each of the foot architectures was optimized to minimize this error by again grid sampling over the range of feasible design variable values.

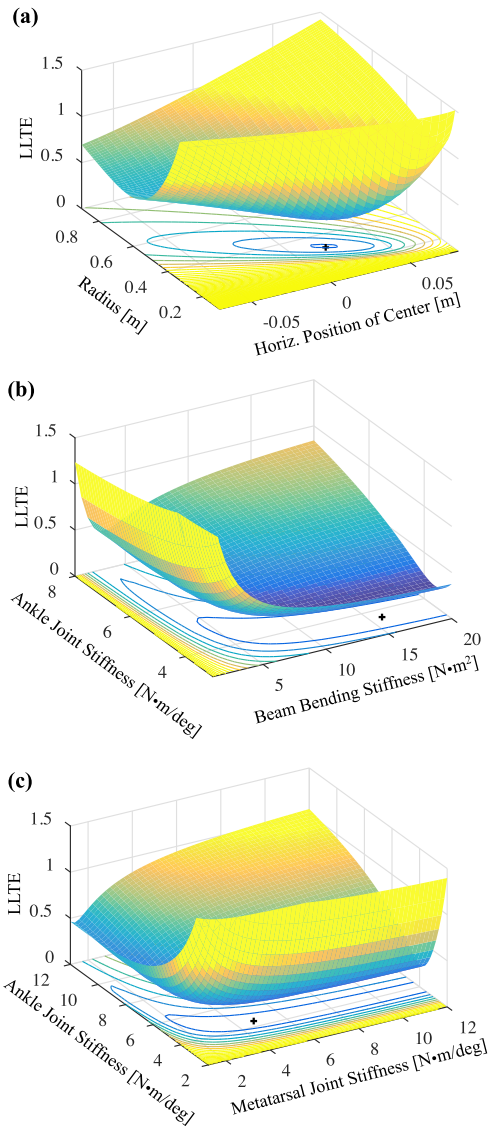

Fig. 6. LLTE values calculated for each conceptual model foot over the prescribed ranges of the design variables: (a) rigid foot, (b) rotational ankle and metatarsal foot, and (c) rotational ankle, beam forefoot foot. The optimal designs are those which produce the minimum LLTE, indicated here by the cross.

D. LLTE Optimization Results

The Lower Leg Trajectory Errors for each of the model foot architectures over the range of design variables considered are shown in Fig. 6. The optimal designs are those with the lowest LLTE values. For the rigid foot model, the optimal design had a radius of 0.32 m and horizontal position of the

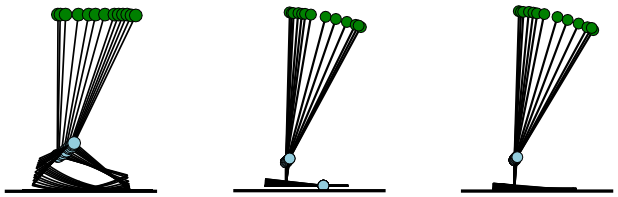

Fig. 7. Lower leg trajectories for LLTE-optimal foot designs from foot flat to late stance. (a) Rigid model. (b) Rotational ankle and metatarsal model. (c) Rotational ankle, beam forefoot model.

center of the circle of 0.02 m, with an LLTE value of 0.292. For the rotational ankle and metatarsal foot, the optimal design had ankle stiffness of 4.4 N·m/deg and metatarsal stiffness of 4.8 N·m/deg, with LLTE value 0.229. For the rotational ankle, beam forefoot foot, the optimal design had ankle stiffness of 3.7 N·m/deg and beam bending stiffness of 16.0 N·m^2, with an LLTE value of 0.222. These LLTE values indicate that the optimal designs for both articulated feet offer a 30% improvement in how well the simulated lower leg kinematics fit the target physiological data over the optimal rigid foot.

To further understand the LLTE value for each of these conceptual architectures, the resulting lower leg trajectories are shown both by depicting the knee-ankle-foot system at equally spaced time intervals during stance phase (Fig. 7), and by examining each of the three spatial coordinates (x_{knee}, y_{knee}, and θ_{LL}) relative to physiological data (Fig. 8).

These results show that while the rigid foot allows the y-coordinate of the knee to replicate the physiological trajectory very closely, the x-coordinate and the orientation of the lower leg differ from the desired physiological trajectory. Consequently, the overall LLTE value is higher than for the other two foot architectures. The lower leg trajectories for both the rotational ankle and metatarsal foot and for the rotational ankle, beam forefoot foot are very similar due to similarities in the articulation of the feet. Consequently, the LLTE values of the optimal designs for each foot are also very close.

Table I summarizes the LLTE- and roll-over-optimal designs and their LLTE values. The LLTE values for the roll-over-optimal rigid foot, rotational ankle and metatarsal foot, and rotational ankle, beam forefoot foot were 0.334, 0.808, and 0.692, respectively, which are much higher than the minimum LLTE values found. Thus the feet optimized for roll-over geometry do not best replicate the physiological lower leg trajectory. The roll-over geometries of both the LLTE- and roll-over optimal designs are shown in Fig. 9. Particularly for the articulated feet, the roll-over optimal designs fit the physiological roll-over shape much better than the LLTE-optimal designs, further illustrating that the design with the best kinematics as measured by the LLTE is not necessarily the design with the best roll-over geometry.

V. Discussion

The presented framework can be used to evaluate feet, optimize design variables for a particular foot architecture, or compare different foot architectures. The LLTE optimization done in the previous section shows that the articulated architectures presented here outperform the rigid circular foot.

It is important to note that the lower leg trajectory error only captures the kinematic and kinetic performance of prosthetic feet. There are many other factors, such as manufacturability, weight, and cost, that must also be considered in early stage foot design. In this case, the rotational ankle, beam forefoot foot would likely be easier to build and lighter weight than the rotational ankle and metatarsal foot, as the cantilever beam requires fewer parts and less structural material than

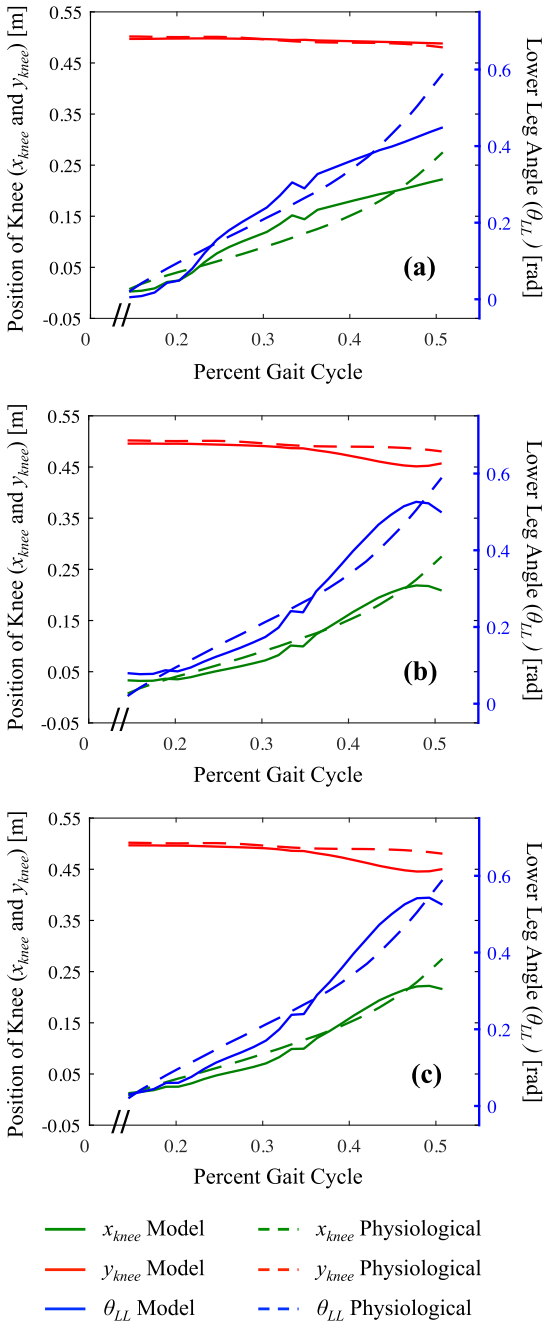

Fig. 8. Individual parameters that make up the LLTE for LLTE-optimal designs: (a) rigid foot, (b) rotational ankle and metatarsal foot, and (c) rotational ankle, beam forefoot foot.

TABLE I
OPTIMAL DESIGN VARIABLES AND LLTE VALUES FOR THE LLTE-OPTIMAL AND ROLL-OVER-OPTIMAL DESIGNS FOR ALL THREE PROSTHETIC FOOT ARCHITECTURES

	LLTE-Optimal Designs			**Roll-Over-Optimal Designs**		
Conceptual Model	Design Variables		LLTE	Design Variables		LLTE
Rigid Foot	R^* = 0.32 m	x_c^* = 0.02 m	0.292	R^* = 0.37 m	x_c^* = 0.00 m	0.334
Rotational Ankle and Metatarsal Foot	k_{ank}^* = 4.4 N·m/deg	k_{met}^* = 4.8 N·m/deg	0.229	k_{ank}^* = 7.0 N·m/deg	$k_{met}^* \to \infty$	0.808
Rotational Ankle, Beam Forefoot	k_{ank}^* = 3.7 N·m/deg	EI^* = 16.0 N·m^2	0.222	k_{ank}^* = 6.3 N·m/deg	EI^* = 25.0 N·m^2	0.692

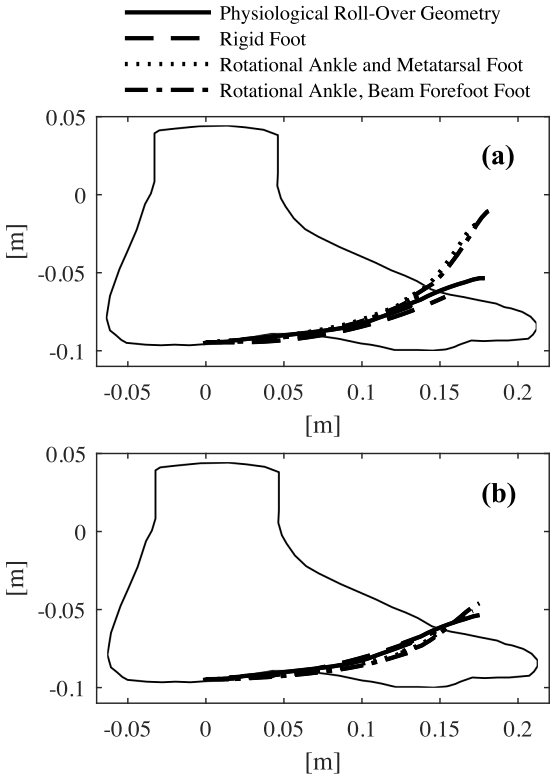

Fig. 9. Roll-over geometries of the LLTE-optimal and the RO-optimal foot designs: (a) LLTE-optimal designs, and (b) roll-over-optimal designs.

the additional rigid link and springs used in the rotational metatarsal joint. The presented framework should be used together with these other factors in early stage prosthetic foot design.

Including the rigid circular foot model in the optimization allows for comparison with Adamczyk's clinical work, in which subjects walked on circular wooden rocker feet with various radii and center located 0.076 m anterior to the ankle-knee segment [21]. He found that the subjects were able to walk most efficiently on feet with radius equal to 30% of their leg length. At $x_c = 0.076$ m, the minimum LLTE occurs for a foot with radius 0.22 m, which is 27% of the leg length of the subject of the gait analysis used in this study. Thus the foot with the optimal LLTE subject to the constraint $x_c = 0.076$ m corresponds closely to the metabolically optimal design as found empirically in Adamczyk's clinical study.

Because the LLTE compares modeled values to physical values at each time interval during a step, it includes a temporal optimization element not present in the roll-over geometry. Most roll-over geometry investigations focus only on the shape itself or certain attributes of the shape, such as radius [3], [4], [21] or arc length [22], [28]. While it is possible to include temporal effects in roll-over geometry by evaluating the rate of progression of the center of pressure, the temporal aspect is not typically considered.

This analysis was performed using inputs from published able-bodied gait data. As previously mentioned, there are differences between the gait of persons with lower limb amputations and able-bodied persons. Additionally, the design of a particular prosthetic foot affects how a user walks. When a prosthetic foot is optimized for able-bodied gait data and then built and tested, there will be differences between the loads actually applied to the prosthesis and the able-bodied loads for which the foot was designed. Consequently, the response of the foot will be different from that predicted in the model.

The authors conducted a clinical study in which a subject with unilateral transtibial amputation walked over flat ground with an experimental foot based on the rotational ankle, beam forefoot architecture discussed here with five different ankle stiffness values [29]. It was found that the able-bodied data were sufficiently close to the data measured during testing with the experimental prototype. This indicates that able-bodied data are appropriate to use as model inputs and target outputs for an LLTE-based foot design. Furthermore, when various aspects of gait mechanics departed from the able-bodied data due to physical limitations in the experimental foot, the contralateral side exhibited compensatory mechanisms at the same time, suggesting that replicating able-bodied kinetics and kinematics may reduce compensatory effects.

As defined here, the error in each of the three variables comprising the lower leg trajectory, x_{knee}, y_{knee} and θ_{LL}, as well as all times throughout the step are weighted as equally as possible in the definition of the optimization parameter LLTE (detailed in Appendix). As this analysis is purely theoretical, there is no reason to suspect that any one of these is more important than the others. In future work, testing should be done to determine whether this is truly the case when a human user is involved, as well as to evaluate alternative cost function definitions, such as using different normalization factors or target data sets.

The proposed optimization parameter, LLTE, only addresses mid-stance kinematics, from foot flat to late stance. The heel strike to foot flat phase of stance can be investigated using the same method, but additional design variables should be added to the models to decouple the early stance and mid to late stance behavior of the foot. Many commercially available prosthetic feet already differentiate the response of the foot

during these two separate phases by using, for example, one cantilever beam extending forward from the ankle and a second cantilever beam extending backward, or a rigid keel forefoot and a foam cushion heel, as in a SACH foot. The heel portion of these prosthetic feet have an additional purpose of providing shock absorption at heel strike.

The model foot architectures investigated in this study are intended only to demonstrate the usefulness of the presented framework of replicating target lower leg trajectories under a set of input loads in prosthetic foot design, and to provide conceptual architectures that could be easily prototyped for clinical validation of this work. The architectures presented are neither exhaustive nor representative of commercially available prosthetic feet. Once this theoretical work has been validated using simple prototypes based off the models discussed here, future work could include expanding the LLTE objective function to more time-intensive optimization problem formulations that will yield designs closer to commercial products, such as designing a single-part compliant mechanism foot [30].

The framework presented here is intended to be used only as a tool for early stage prosthetic foot design and analysis. In clinically evaluating existing feet, all of the resulting data, both kinematic and kinetic, must be measured. In the course of this work, kinetic data has been used as an input and kinematic data as an output, but in a clinical context it may be found that a person walks with near perfect gait kinematics with a foot with a very high LLTE value, but in order to do so the kinetics must deviate significantly from normative data. For a foot with a very low LLTE value, kinematic data close to the target kinematics will only be possible with kinetics close to those used as inputs, and vice versa. For such a foot with a low LLTE value, it is expected that both the kinematics and kinetics measured clinically will be close to those values used in the optimization process, as has been demonstrated in [29].

VI. Conclusion

This work presents a novel framework that quantitatively connects the mechanical design of a prosthetic foot to its anticipated biomechanical performance. The framework uses kinetic inputs to predict kinematic outputs of the lower leg by knowing the geometry and stiffness of the foot. The error between the output kinematics and the target kinematics is evaluated using a root-mean-square error function that we call the Lower Leg Trajectory Error (LLTE). The LLTE can be used as an optimization parameter to tune the stiffness of a foot to produce accurate lower leg kinematics. The framework is agnostic to a specific foot design, as long as the constitutive behavior of the foot can be characterized. In this study, physiological kinetics were used as the input to the framework, with physiological kinematics as the targets; the framework is flexible and could accept alternate inputs and targets, depending on what performance and clinical objectives are desired.

Three model foot architectures were optimized using the LLTE-based framework. The results were compared to the same models optimized for roll-over geometries. It was shown that the feet with roll-over geometries closest to physiological do not necessarily result in the best lower leg kinematics. Roll-over geometry omits the kinematic constraint between a specific foot design and the ground, the orientation of the lower leg, and the temporal progression of the step – important parameters for both gait kinematics and joint reaction forces and moments. Consequently, it is possible for a prosthetic foot to exactly mimic the physiological roll-over shape, but greatly differ from physiological lower leg orientation. While further testing is required to validate the full clinical effectiveness of the Lower Leg Trajectory Error, incorporating more information than the roll-over geometry alone into the design of passive prostheses will facilitate improved replication of physiological gait.

Appendix

The focus of this work is the novel framework of predicting the lower leg trajectory for a modeled prosthetic foot and comparing that trajectory to a target lower leg trajectory, thereby creating a prosthesis that seamlessly integrates into the body's natural motion and loading. In order to use this approach to optimize prosthetic feet, it was necessary to define a particular cost function, that given in Eq. (1). As is often the case in formulating optimization problems, there are an infinite number of potential cost functions that could be used to quantify the difference between a modeled and physiological lower leg trajectory. Clinical studies, such as that performed by the authors in conjunction with this work [29], are required to better inform the definition of this cost function. In the absence of clinical evidence at the time of writing, the authors have defined the cost function to provide what they believe is the most logical comparison between modeled and targeted data. The rationale for the definition of the cost function as defined in this work is described here.

Exactly three independent variables define the position of a line segment in two-dimensional space. There are an infinite number of variables that could be chosen to define the position of the lower leg segment at each time, but if more than three are used, any variables beyond the initial three can always be defined in terms of these three variables and constants inherent to the problem. For example, if the x- and y-positions of both the ankle and the knee were selected (four variables total), the y-position of the knee could be written as

$$y_{knee} = y_{ank} + \sqrt{L_{shank}^2 - (x_{knee} - x_{ank})^2}, \qquad (18)$$

where L_{shank} is the length of the lower leg segment, which remains constant. Writing y_{knee} in terms of x_{ank}, y_{ank}, and x_{knee} shows that y_{knee} is a dependent variable rather than a fourth independent variable.

Of the infinite number of possibilities, two sets of three independent variables were identified by the authors as the most intuitive: (1) the x- and y- position of the ankle joint and the angular orientation of the lower leg segment with respect to vertical, and (2) the x- and y- position of the knee joint and the angular orientation of the lower leg segment with respect to vertical. These sets of variables were selected because markers are typically placed on the ankle and knee during gait analysis studies, so data for the position of these two

anatomical positions are readily available without additional post-processing. The angle of the lower leg segment with respect to vertical was included as the third variable because it was more logical to the authors to use the angle rather than one or the other of the x and y positions of either the ankle or knee joint as the third variable. In the ICORR paper that first presented this framework, the lower leg trajectory was defined using the position of the ankle and the orientation of the lower leg segment [23]. In the time since that work was published, the authors reached the conclusion that the knee was a preferable reference point, as the motion at the knee is much larger than the motion at the ankle during stance phase, so any differences in position are magnified at the knee relative to the ankle. Additionally, a person with a transtibial amputation receives direct feedback from his or her biological knee joint and consequently may be more sensitive to kinematic differences at the knee than at the ankle.

Regardless of the variables chosen, a normalization factor must be used to evaluate the cumulative distance between two data sets containing three different variables. Even if the variables have the same units, such as the x- and y-positions of the knee joint, a normalization factor is necessary to provide context for the difference between modeled and measured data, as a difference of 5 cm may not be much for the x-position of the knee, which moves a total of 26 cm during controlled dorsiflexion, but may be substantial for the y-position of the knee, which moves 2 cm in the same time period. Therefore, regardless of the choice of variables used to define the position of the lower leg segment, it will always be necessary to select a normalization factor.

The most common normalization factors in comparing model-predicted values to a measured data set (the physiological gait data in this context) are the mean of the measured data set, the range of the measured data set, or the individual data point values. In Eq. (1), the physiological mean is used as the normalization factor. If the range or individual data point values were used instead, the cost function equation would become

$$LLTE \equiv \left[\frac{1}{N}\sum_{n=1}^{N}\left\{\left(\frac{x_{knee,n}^{model}-x_{knee,n}^{phys}}{\max\left(x_{knee}^{phys}\right)-\min\left(x_{knee}^{phys}\right)}\right)^2+\left(\frac{y_{knee,n}^{model}-y_{knee,n}^{phys}}{\max\left(y_{knee}^{phys}\right)-\min\left(y_{knee}^{phys}\right)}\right)^2+\left(\frac{\theta_{LL,n}^{model}-\theta_{LL,n}^{phys}}{\max\left(\theta_{knee}^{phys}\right)-\min\left(\theta_{knee}^{phys}\right)}\right)^2\right\}\right]^{\frac{1}{2}} \quad (19)$$

or

$$LLTE \equiv \left[\frac{1}{N}\sum_{n=1}^{N}\left\{\left(\frac{x_{knee,n}^{model}-x_{knee,n}^{phys}}{x_{knee,n}^{phys}}\right)^2+\left(\frac{y_{knee,n}^{model}-y_{knee,n}^{phys}}{y_{knee,n}^{phys}}\right)^2+\left(\frac{\theta_{LL,n}^{model}-\theta_{LL,n}^{phys}}{\theta_{LL,n}^{phys}}\right)^2\right\}\right]^{\frac{1}{2}}. \quad (20)$$

Ideally, the normalization factors serve the purpose of weighting each term in the above equations as equally as possible, both in time over the course of the step, and in each of the three variables, x_{knee}, y_{knee}, and θ_{LL}. In our previous ICORR publication, the physiological range was used as the normalization factor. This was appropriate with the x- and y-position of the ankle defining the lower leg position, since the range for both variables was similarly small. However, the x-position of the knee and the angular orientation of the lower leg segment vary much more than the y-position of the knee during stance. Consequently, the normalization factor for the y-term in Eq. (19) was very small, causing the y-term to dominate the LLTE value for a given design, which resulted in an optimal design that replicated the y-position of the physiological knee very closely, but were far from the x-position of the knee and the angular orientation of the lower leg, as shown in Fig. 10a for the rotational ankle and metatarsal foot architecture.

Ultimately, normalizing by physiological means was chosen in this work rather than by individual physiological data point

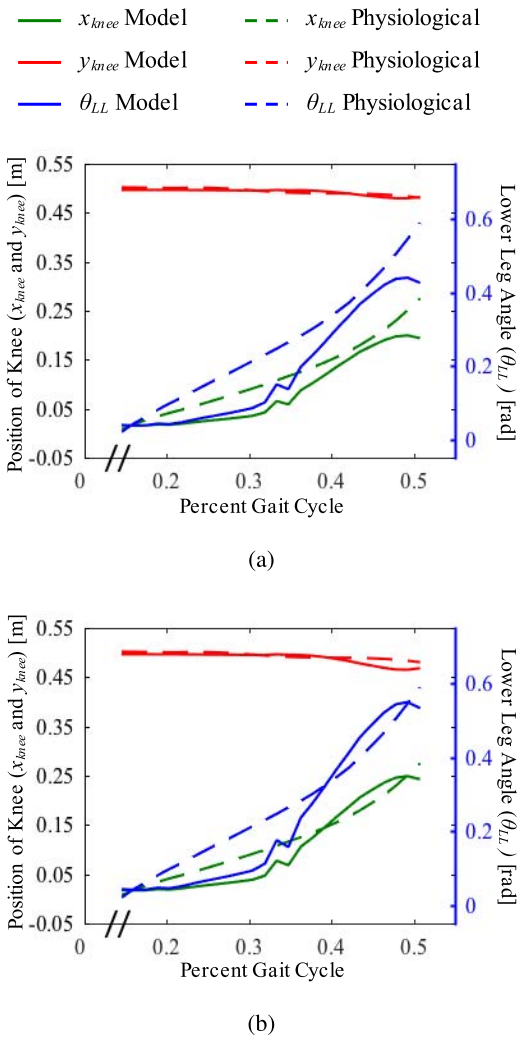

Fig. 10. x_{knee}, y_{knee}, and θ_{LL} for optimal designs for the rotational ankle and metatarsal foot architecture using cost functions with terms normalized by (a) physiological range (Eq. (19), k^*_{ank} = 9.0 N · m/deg, k^*_{met} = 2.2 N · m/deg) and (b) physiological data point values (Eq. (20), k^*_{ank} = 8.2 N · m/deg, k^*_{met} = 1.6 N · m/deg). The error was distributed better both in time across the step and between each of the three spatial variables when the physiological mean was used as the normalization factor, as in Eq. (1) (Fig. 8b).

values, as the optimal designs more closely replicated all three variables throughout the entire step, particularly toward the beginning of the controlled dorsiflexion phase, as shown in comparing Fig. 10b to Fig. 8b.

As previously stated, it is necessary to define a cost function, such as that in Eq. (1), to design feet using this framework, which can then be used to evaluate and refine the framework, and, in particular, the cost function definition. Such work requires substantial time and effort, but cannot begin without an initial definition of the cost function. The authors encourage other researchers to employ this framework with variations on the cost function. Regardless of the exact cost function definition, the framework presented here provides a means to connect the mechanical design of a prosthetic foot to its biomechanical functionality in terms of kinetics and kinematics, that will aid in understanding differences observed when multiple prosthetic feet of different mechanical designs are compared.

Acknowledgment

The authors would like to thank Mr. D. R. Mehta, Dr. Pooja Mukul, and Dr. M. K. Mathur at Bhagwan Mahaveer Viklang Sahayata Samiti for their partnership and support.

References

[1] P. G. Adamczyk and A. D. Kuo, "Mechanisms of gait asymmetry due to push-off deficiency in unilateral amputees," *IEEE Trans. Neural Syst. Rehabil. Eng.*, vol. 23, no. 5, pp. 776–785, Sep. 2014.

[2] K. E. Zelik *et al.*, "Systematic variation of prosthetic foot spring affects center-of-mass mechanics and metabolic cost during walking," *IEEE Trans. Neural Syst. Rehabil. Eng.*, vol. 19, no. 4, pp. 411–419, Aug. 2011.

[3] E. Klodd, A. Hansen, S. Fatone, and M. Edwards, "Effects of prosthetic foot forefoot flexibility on gait of unilateral transtibial prosthesis users," *J. Rehabil. Res. Develop.*, vol. 47, no. 9, pp. 899–910, 2010.

[4] E. Klodd, A. Hansen, S. Fatone, and M. Edwards, "Effects of prosthetic foot forefoot flexibility on oxygen cost and subjective preference rankings of unilateral transtibial prosthesis users," *J. Rehabil. Res. Develop.*, vol. 47, no. 6, pp. 543–552, 2010.

[5] K. Postema, H. Hermens, J. De Vries, H. Koopman, and W. Eisma, "Energy storage and release of prosthetic feet, Part 1: Biomechanical analysis related to user benefits," *Prosthetics Orthotics Int.*, vol. 21, no. 1, pp. 17–27, 1997.

[6] M. J. Major, M. Twiste, L. P. Kenney, and D. Howard, "The effects of prosthetic ankle stiffness on ankle and knee kinematics, prosthetic limb loading, and net metabolic cost of trans-tibial amputee gait," *Clin. Biomech.*, vol. 29, no. 1, pp. 98–104, 2014.

[7] N. P. Fey, G. K. Klute, and R. R. Neptune, "Optimization of prosthetic foot stiffness to reduce metabolic cost and intact knee loading during below-knee amputee walking: A theoretical study," *J. Biomech. Eng.*, vol. 134, no. 11, p. 111005, 2012.

[8] N. P. Fey, G. K. Klute, and R. R. Neptune, "Altering prosthetic foot stiffness influences foot and muscle function during below-knee amputee walking: A modeling and simulation analysis," *J. Biomech. Eng.*, vol. 46, no. 4, pp. 637–644, 2013.

[9] C. Hofstad, H. van der Linde, J. van Limbeek, and K. Postema, "Prescription of prosthetic ankle-foot mechanisms after lower limb amputation (Cochrane Review)," in *Cochrane Library*, no. 1. Chichester, U.K.: Wiley, 2004.

[10] H. van der Linde *et al.*, "A systematic literature review of the effect of different prosthetic components on human functioning with a lower-limb prosthesis," *J. Rehabil. Res. Develop.*, vol. 41, no. 4, pp. 555–570, 2004.

[11] B. J. Hafner, "Clinical prescription and use of prosthetic foot and ankle mechanisms: A review of the literature," *J. Prosthetics Orthotics*, vol. 17, no. 4, pp. S5–S11, 2005.

[12] M. J. Major, L. P. Kenney, M. Twiste, and D. Howard, "Stance phase mechanical characterization of transtibial prostheses distal to the socket: A review," *J. Rehabil. Res. Develop.*, vol. 49, no. 6, pp. 815–829, 2012. [Online]. Available: http://www.ncbi.nlm.nih.gov/pubmed/23299254

[13] H. W. L. Van Jaarsveld, H. J. Grootenboer, J. de Vries, and H. F. Koopman, "Stiffness and hysteresis properties of some prosthetic feet," *J. Prosthetics Orthotics*, vol. 14, no. 3, pp. 117–124, Dec. 1990. [Online]. Available: http://www.ncbi.nlm.nih.gov/pubmed/2095529

[14] H. Lee, E. J. Rouse, and H. I. Krebs, "Summary of human ankle mechanical impedance during walking," *IEEE J. Transl. Eng. Health Med.*, vol. 4, 2016, Art. no. 2100407.

[15] G. J. V. D. Water, J. de Vries, and M. Mulder, "Comparison of the lightweight camp normal activity foot with other prosthetic feet in transtibial amputees: A pilot study," *Prosthetics Orthotics Int.*, vol. 22, no. 2, pp. 107–114, 1998.

[16] M. D. Geil, "Energy loss and stiffness properties of dynamic elastic response prosthetic feet," *J. Prosthetics Orthotics*, vol. 13, no. 3, pp. 70–73, 2001.

[17] M. D. Geil, "An iterative method for viscoelastic modeling of prosthetic feet," *J. Biomech.*, vol. 35, no. 10, pp. 1405–1410, 2002.

[18] N. P. Fey, G. K. Klute, and R. R. Neptune, "The influence of energy storage and return foot stiffness on walking mechanics and muscle activity in below-knee amputees," *Clin. Biomech.*, vol. 26, no. 10, pp. 1025–1032, 2011.

[19] J. D. Ventura, G. K. Klute, and R. R. Neptune, "The effect of prosthetic ankle energy storage and return properties on muscle activity in below-knee amputee walking," *Gait Posture*, vol. 33, no. 2, pp. 220–226, 2011.

[20] A. H. Hansen, D. S. Childress, and E. H. Knox, "Prosthetic foot roll-over shapes with implications for alignment of transtibial prostheses," *Prosthetics Orthotics Int.*, vol. 24, no. 3, pp. 205–215, Jan. 2000. [Online]. Available: http://poi.sagepub.com/lookup/doi/10.1080/03093640008726549

[21] P. G. Adamczyk, S. H. Collins, and A. D. Kuo, "The advantages of a rolling foot in human walking," *J. Exp. Biol.*, vol. 209, no. 20, pp. 3953–3963, Oct. 2006. [Online]. Available: http://www.ncbi.nlm.nih.gov/pubmed/17023589

[22] P. G. Adamczyk and A. D. Kuo, "Mechanical and energetic consequences of rolling foot shape in human walking," *J. Exp. Biol.*, vol. 216, no. 14, pp. 2722–2731, Jul. 2013. [Online]. Available: http://www.ncbi.nlm.nih.gov/pubmed/23580717

[23] K. M. Olesnavage and A. G. V. Winter, "Lower leg trajectory error: A novel optimization parameter for designing passive prosthetic feet," in *Proc. IEEE Int. Conf. Rehabil. Robot. (ICORR)*, Aug. 2015, pp. 271–276.

[24] D. A. Winter, *Biomechanics and Motor Control of Human Movement*, 4th ed. Hoboken, NJ, USA: Wiley, 2009.

[25] M. L. Handford and M. Srinivasan, "Robotic lower limb prosthesis design through simultaneous computer optimizations of human and prosthesis costs," *Sci. Rep.*, vol. 6, Feb. 2016, Art. no. 19983.

[26] R. Gailey, K. Allen, J. Castles, J. Kucharik, and M. Roeder, "Review of secondary physical conditions associated with lower-limb amputation and long-term prosthesis use," *J. Rehabil. Res. Develop.*, vol. 45, no. 1, p. 15, 2008.

[27] L. L. Howell, *Compliant Mechanisms*. Hoboken, NJ, USA: Wiley, 2001.

[28] A. H. Hansen, M. R. Meier, P. H. Sessoms, and D. S. Childress, "The effects of prosthetic foot roll-over shape arc length on the gait of trans-tibial prosthesis users," *Prosthetics Orthotics Int.*, vol. 30, no. 3, pp. 286–299, Dec. 2006. [Online]. Available: http://www.ncbi.nlm.nih.gov/pubmed/17162519

[29] K. M. Olesnavage, "Development and validation of a novel framework for designing and optimizing passive prosthetic feet using lower leg trajectory," Ph.D. dissertation, Dept. Mech. Eng., Massachusetts Inst. Technol., Cambridge, MA, USA, Feb. 2018.

[30] K. M. Olesnavage and A. G. V. Winter, "Passive prosthetic foot shape and size optimization using lower leg trajectory error," in *Proc. ASME Int. Design Eng. Techn. Conf. (IDETC)*, 2017, pp. V05AT08A011-1–V05AT08A011-10, doi: 10.1115/DETC2017-67618.